# A Novel Computational Sheep Atria Model for the Study of Atrial Fibrillation

Timothy D Butters[1], Jichao Zhao[2], Bruce Smaill[2], Henggui Zhang[1]

[1]School of Physics and Astronomy, University of Manchester, Manchester, UK
[2]Auckland Bioengineering Institute, University of Auckland, Auckland, NZ

## Abstract

*Sheep is an animal model often used for experimental studies into the underlying mechanisms of cardiac arrhythmias. Previous studies have shown that biophysically detailed computer models of the heart provide a powerful alternative to experimental animal models for underpinning such mechanisms. In this study we have developed a family of mathematical models for the electrical action potentials of various sheep atrial cell types. We have also developed a 3D model for the anatomical structure of the sheep atria. By incorporating the single cell models into the anatomical structure, a novel computational model for the sheep atria has been reconstructed. This model was then used to investigate the mechanisms by which rapid focal activity in the pulmonary veins can transit to atrial fibrillation. It was found that the anisotropic property of the atria arising from the fibre structure plays an important role in facilitating fibrillatory atrial excitation waves.*

## 1. Introduction

Atrial fibrillation (AF) is the most common sustained arrhythmia in the developed world, affecting approximately 1.5% of its population [1]. The prevalence of AF increases with age, therefore in an ageing population AF is set to become a leading factor in mortality, morbidity and quality of life of the general population [2, 3]. Although AF is a common arrhythmia its genesis is not well understood, therefore further studies to better understand its causes are paramount. Sheep are often used as experimental animal models to study cardiac diseases such as atrial fibrillation [4–8]. However, there are currently no species-specific mathematical models for the sheep atria that can help interpret these data using integrative system biology approaches.

In this study we have developed a new family of mathematical models for the electrical action potentials (APs) of different cell types of the sheep atria: the pectinate muscles (PM), crista terminalis (CT), right atrial appendage (RAA), Bachmann's bundle (BB), the left atrium (LA) and the pulmonary veins (PV). These single cell models take into account the experimentally observed electrical heterogeneity of sheep atrial cells in the kinetics and current densities of their ion channels. The models were based on, and validated against, extant experimental data from sheep atrial cells. In the cases where no experimental data was available cross-species modelling techniques were utilised.

We have also reconstructed a 3D anatomical model of the sheep atria using extended volume imaging [9]. This reconstruction includes details of the complex fibre structure of the atria, and is segmented into the different atrial regions.

The developed single cell models were then incorporated into an anatomically detailed reconstruction of a sheep atria. This provided a computational platform that could be used to investigate the genesis of AF and the importance of electrical heterogeneity and fibre structure on its development and sustainability.

## 2. Methods

### 2.1. Developing single cell models

The Ramirez *et al.* mathematical models of the canine atrium were used as a base for the new sheep models [10]. This model set includes detailed descriptions of cells in the right atrium (RA), but do not include models for the fast conduction pathway of BB, the LA, or the PVs. In this study, the Ramirez *et al.* model set was first expanded to describe these cell types using detailed experimental data from Li *et al.*, Ehrlich *et al.* and Burashnikov *et al.* [11–13]. These models were then used as a base to produce a full set of APs for the sheep atria using recorded AP data from Lenaerts *et al.* [14].

Experimental voltage clamp and action potential data for canine LA and PV cells has been published by Li *et al.* and Ehrlich *et al.* [11, 12], and detailed action potential data of BB in the canine atria was available from Burashnikov *et al.* [13]. This allowed for accurate species specific models of these cell types to be created. Fig. 1 shows the fitted ionic current data for the left atrial and pulmonary vein cells.

To create species-specific models of the sheep atria the

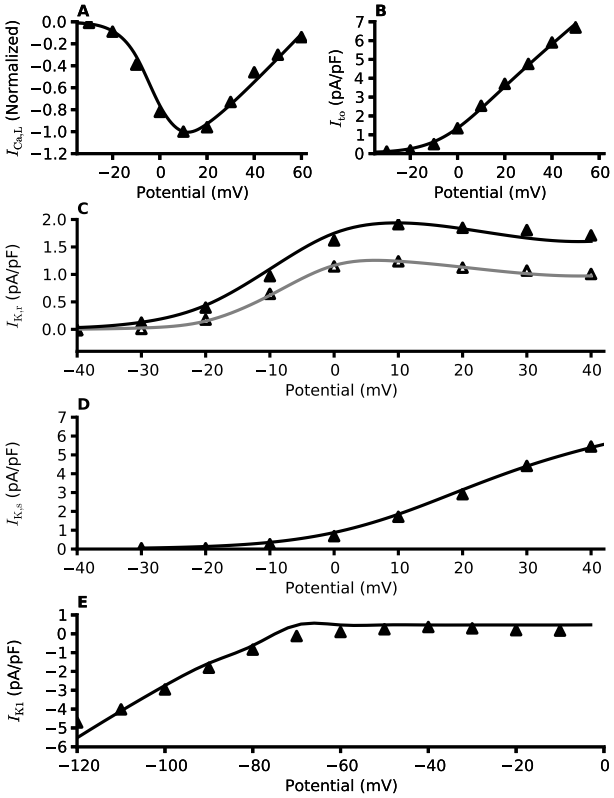


Figure 1. Simulated current-voltage relationships with experimental data for canine atrial cells. Closed triangles represent data from Ehrlich et al. [12], open triangles represent data from Li et al. [11].

parameters of the RAA canine cell model were altered so that the simulated AP morphology matched experimentally recorded APs from Lenaerts *et al.* [14]. It was then assumed that the same ionic changes used to differentiate between different cell types of the canine atria would apply to the sheep atria. This produced a full set of mathematical models for the sheep atria, shown in Fig. 2.

## 2.2. Developing the 3D atria model

The 3D sheep atria geometry was reconstructed using extended volume imaging [9]. The tissue was set in resin, then imaged at 50 $\mu$m intervals using a high resolution camera with an in-plane resolution of 50 $\mu$m [15]. The complex fibre structure of the tissue was extracted using 3D eigen-analysis of the structure tensor constructed from the image volume [15]. The reconstruction of the fibre architecture allowed the tissue to be segmented into the different atrial regions by identifying the organised structures of BB, the CT and the PMs, and the change in fibre orientation around the PV region.

The AP propagation throughout the tissue was simulated using the monodomain reaction-diffusion equation [16].

$$\frac{\partial V}{\partial t} = \nabla \cdot (\mathbf{D} \nabla V) - \frac{I_{\text{ion}}}{C_m}. \quad (1)$$

Where $V$ is the membrane potential, $t$ is time, $\mathbf{D}$ is the diffusion tensor describing the AP spread in relation to the orientation of the myofibres, $I_{\text{ion}}$ is the total ionic membrane current and $C_m$ is the capacitance of the cell membrane. $I_{\text{ion}}$ is calculated for each cell in the tissue, and varies between different cell types. Values for the diffusion coefficients that make up the diffusion tensor, $\mathbf{D}$, were chosen so that the produced activation time and conduction velocities of the atria match those measured experimentally. The simulations used a finite difference numerical scheme using a forward Euler integration method with time and space steps of 0.005 ms and 0.3 mm respectively.

## 2.3. Investigating mechanisms of AF

The arrhythmogenic properties of the PV region were investigated, in particular, the genesis of AF through rapid spontaneous excitation from the PV sleeves. A series of short-coupled stimuli (3 stimuli with a cycle length of 100 ms) were given to a small section of the sleeve of the right anterior PV. After this point no more excitations were given to the tissue. This was carried out for three cases, the first considered both the electrical heterogeneity and the complex fibre structure of the atria. Each cell type in the tissue was simulated using the appropriate AP model, and preferential conduction was modelled along the direction of the myofibres. The second case considered only the electrical heterogeneity, ignoring the myofibre architecture. In this simulation the conduction was isotropic. The third case included anisotropic conduction, but the whole tissue was simulated using the AP model of the RAA, ignoring the electrical heterogeneity of the atria.

# 3. Results

## 3.1. 3D sheep atria

Simulated APs from the developed sheep atria models are shown in Fig. 2. As can be seen in panel A, the AP simulation from the RAA matches well with the experimental recording from Lenaerts *et al.* [14]. The APs from the other cell types in the atria show the same relative morphological differences (such as $\text{APD}_{90}$, resting potential and amplitude) as those found in other mammalian atrial models such as the canine and rabbit [10, 13, 16].

The AP models were then incorporated into the 3D atrial geometry, with conduction velocities in the atria be-

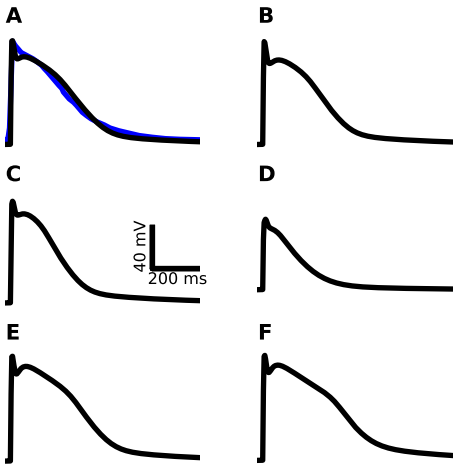


Figure 2. Simulated action potentials from the developed sheep models for the atrial appendage (A), pectinate muscles (B), left atrium (C), pulmonary veins (D), crista terminalis (E) and Bachmann's bundle (F). The blue line in (A) shows the experimentally recorded sheep action potential from Lenaerts *et al.* [14]

tween 0.8 – 1.5 m/s, with the fastest conduction being seen along BB. These results are consistent with experimental conduction velocity measurements from the sheep atria [17–19]. As well as BB, preferential conduction is also seen along other organised fibre structures such as the CT and PMs.

## 3.2. Investigating AF

It was found that AF could be initiated with the pacing protocol outlined in section 2.3 both with and without the complex fibre orientation. However, it was not possible to initiate AF without considering the electrical heterogeneity of the atria. In the cases where it was possible to initiate AF, re-entry first occurred around the sleeves of the PVs. After a few seconds the re-entrant excitation waves would breakdown further and re-entry either within or around one or more of the atria was seen. Fig. 3 shows typical fibrillatory patterns for the two successful cases. As can be seen from this figure, the fibrillatory patterns are considerably different between the two cases. When the fibre structure was considered the waves breakdown into a more irregular pattern (Fig. 3Ai-Aiii), with a mother rotor in the left atrium that drives the fibrillation. The mother rotor persisted for the duration of the simulation (10 s). Without the fibre structure (Fig. 3Bi-Biii) wavelets with a larger wavelength are seen with more homogeneous patterns, with constant re-entry occurring around both atria.

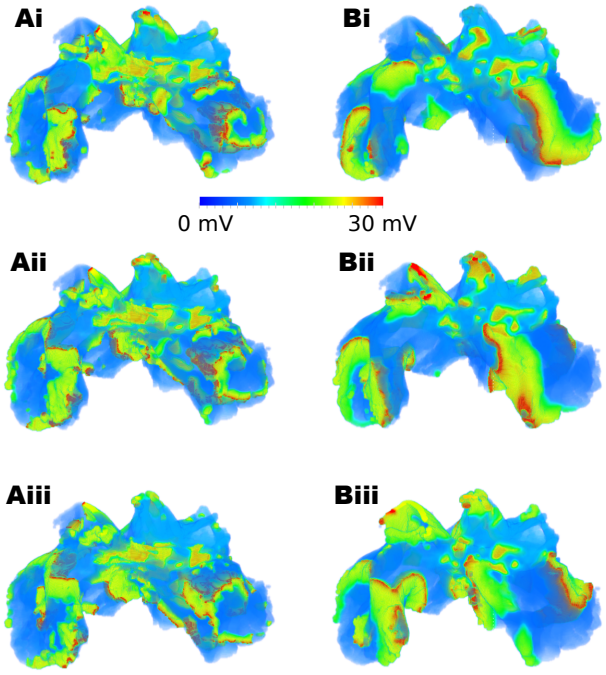


Figure 3. Simulated atrial fibrillation in the 3D sheep atria at 5 ms intervals (superior-anterior view), with (A) and without (B) consideration of the complex fibre orientation. From 7000 ms simulation time (i) to 7010 ms (iii).

## 4. Discussion and conclusions

A biophysically detailed computational model of the 3D sheep atria has been created, which includes species-specific models of the sheep atrial myocytes. These are consistent with experimental measurements of electrophysiological details such as AP properties [14] and conduction velocities [17–19].

This model has been used to investigate the initiation of AF through rapid stimuli in the PV region, and the development of fibrillation within the atria. It is clear that AF can be initiated through spontaneous activity in the PV region, with simulations showing AF both with and without the complex fibre structure of the atria. However, it is also clear that the fibre structure plays an important role in the development of AF. When the fibre structure was ignored regular re-entrant patterns were seen, with large re-entrant wavelets (Fig. 3B). When the fibre structure was considered the fibrillatory waves broke down further, with multiple small wavelets throughout the tissue (Fig. 3A). A mother rotor is seen in the LA which appears to drive the fibrillation. This could occur because the fibre structure

in the LA is much more homogeneous compared to the complex structures of the PV region and the RA, which contains the CT and PMs. The highly anisotropic conduction caused by these structures could cause the rapid breakdown of re-entrant waves, and would account for the irregular fibrillatory patterns seen in this case.

In conclusion, we have developed a novel biophysically detailed model for the 3D sheep atria that considered electrical heterogeneity and anatomical anisotropy. The model provides a powerful tool for investigating the mechanisms underlying cardiac arrhythmias, as well as the actions of pharmacological agents on atrial excitation.

## Acknowledgements

This work was supported by the Engineering and Physical Sciences Research Council UK and the Health Research Council of New Zealand.

## References

[1] Lip GYH, Kakar P, Watson T. Atrial fibrillation – the growing epidemic. Heart 2007;93(5):542–543.

[2] Thrall G, Lane D, Carroll D, Lip GYH. Quality of life in patients with atrial fibrillation: A systematic review. Am J Med 2006;119(5):e1–e19.

[3] Freestone B, Lip GYH. Epidemiology and costs of cardiac arrhythmias. Cardiac Arrhythmias a clinical approach Edinburgh 2003;3–24.

[4] Tanaka K, Zlochiver S, Vikstrom KL, Yamazaki M, Moreno J, Klos M, Zaitsev AV, Vaidyanathan R, Auerbach DS, Landas S, Guiraudon G, Jalife J, Berenfeld O, Kalifa J. Spatial distribution of fibrosis governs fibrillation wave dynamics in the posterior left atrium during heart failure. Circ Res 2007;101(8):839–847.

[5] Tsamis A, Bothe W, Kvitting JP, Swanson JC, Miller DC, E. K. Active contraction of cardiac muscle: In vivo characterization of mechanical activation sequences in the beating heart. J Mech Behav Biomed Mater 2011;4(7):1167–1176.

[6] Mower MM, Hepp D, Hall R. Comparison of chronic biphasic pacing versus cathodal pacing of the right ventricle on left ventricular function in sheep after myocardial infarction. Ann Noninvasive Electrocardiol 2011;16(2):111–116.

[7] Squara P, Borenstein N, Daniel P. Hemodynamic exercise testing and hormonal status in a sheep model of congestive heart failure. Minerva Anestesiol 2011;77(3):283–291.

[8] Berenfeld O, Ennis S, Hwang E, Hooven B, Grzeda K, Mironov S, Yamazaki M, Kalifa J, Jalife J. Time- and frequency-domain analyses of atrial fibrillation activation rate: The optical mapping reference. Heart Rhythm 2011; 8(11):1758–1765.

[9] Sands GB, Gerneke DA, Smaill BH, Legrice IJ. Automated extended volume imaging of tissue using confocal and optical microscopy. 28th Annual International Conference of the IEEE 2006;133–136.

[10] Ramirez RJ, Nattel S, Courtemanche M. Mathematical analysis of canine atrial action potentials: rate, regional factors, and electrical remodelling. Am J Physiol Heart Circ Physiol 2000;279:H1767–H1785.

[11] Li D, Zhang L, Kneller J, Nattel S. Potential ionic mechanism for repolarization differences between canine right and left atrium. Circ Res 2001;88:1168–1175.

[12] Ehrlich JR, Cha TJ, Zhang L, Chartier D, Melnyk P, Hohnloser SH, Nattel S. Cellular electrophysiology of canine pulmonary vein cardiomyocytes: action potential and ionic current properties. J Physiol 2003;551(Pt 3):801–813.

[13] Burashnikov A, Mannava S, Antzelevitch C. Transmembrane action potential heterogeneity in the canine isolated arterially perfused right atrium: effect of ikr and ikur/ito block. Am J Physiol Heart Circ Physiol 2004;286:H2393–H2400.

[14] Lenaerts I, Bito V, Heinzel FR, Driesen RB, Holemans P, D'Hooge J, Heidbüchel H, Sipido KR, Willems R. Ultrastructural and functional remodeling of the coupling between $Ca^{2+}$ influx and sarcoplasmic reticulum $Ca^{2+}$ release in right atrial myocytes from experimental persistent atrial fibrillation. Circ Res 2009;105:876–885.

[15] Zhao J, Butters TD, Zhang H, Pullan AJ, LeGrice IJ, Sands GB, Smaill BH. An image-based model of atrial muscular architectureclinical perspective effects of structural anisotropy on electrical activation. Circ Arrhythm Electrophysiol 2012;5(2):361–370.

[16] Aslanidi OV, Boyett MR, Dobrzynski H, Li J, Zhang H. Mechanisms of transition from normal to reentrant electrical activity in a model of rabbit atrial tissue: Interaction of tissue heterogeneity and anisotropy. Biophys J 2009; 96:798–817.

[17] Klos M, Calvo D, Yamazaki M, Zlochiver S, Mironov S, Cabrera JA, Sanchez-Quintana D, Jalife J, Berenfeld O, Kalifa J. Atrial septopulmonary bundle of the posterior left atrium provides a substrate for atrial fibrillation initiation in a model of vagally mediated pulmonary vein tachycardia of the structurally normal heart. Circ Arrhythm Electrophysiol 2008;1(3):175–183.

[18] Morton JB, Byrne MJ, Power JM, Raman J, Kalman JM. Electrical remodeling of the atrium in an anatomic model of atrial flutter: relationship between substrate and triggers for conversion to atrial fibrillation. Circulation 2002; 105(2):258–264.

[19] Lau DH, Psaltis PJ, Mackenzie L, Kelly DJ, Carbone A, Worthington M, Nelson AJ, Zhang Y, Kuklik P, Wong CX, Edwards J, Saint DA, Worthley SG, Sanders P. Atrial remodeling in an ovine model of anthracycline-induced nonischemic cardiomyopathy: remodeling of the same sort. J Cardiovasc Electrophysiol 2011;22(2):175–182.

Address for correspondence:

Dr. Timothy Butters
Room 3.08 / The Schuster Laboratory
The University of Manchester
Oxford Road / Manchester
UK / M13 9PL
timothy.butters@postgrad.manchester.ac.uk